International Journal of Modern Physics B
Vol. 23, Nos. 12 & 13 (2009) 2647–2654

World Scientific
www.worldscientific.com

TRANSPARENCY OF NARROW CONSTRICTIONS IN A GRAPHENE SINGLE ELECTRON TRANSISTOR

C. STAMPFER†, E. SCHURTENBERGER , F. MOLITOR, J. GÜTTINGER, T. IHN and K. ENSSLIN

Solid State Physics Laboratory ETH Zurich, 8093, Zurich, Switzerland
† *stampfer@phys.ethz.ch*

Received 21 August 2008

We report on electronic transport experiments on a graphene single electron transistor as function of a perpendicular magnetic field. The device, which consists of a graphene island connected to source and drain electrodes via two narrow graphene constrictions is electronically characterized and the device exhibits a characteristic charging energy of approx. 3.5 meV. We investigate the homogeneity of the two graphene "tunnel" barriers connecting the single electron transistor to source and drain contacts as function of laterally applied electric fields, which are also used to electrostatically tune the overall device. Further, we focus on the barrier transparency as function of an applied perpendicular magnetic field and we find an increase of transparency for increasing magnetic field and a source-drain current saturation for magnetic fields exceeding 5 T.

Keywords: Graphene; Single Electron Transistors; Quantum Dots; Mesoscopic Physics.

1. Introduction

Graphene nanostructures[1-7] and in particular graphene quantum dots[6,7] are attracting increasing attention, mainly due to unique electronic properties of the truly two-dimensional (2D) character of graphene.[8] Primarily, the potentially weak spin-orbit interaction and hyperfine coupling in graphene[9,10] leads to promising long spin coherence times making this material system interesting for solid-state, quantum dot based spin-qubit applications.[11] Intrinsic difficulties in confining electrons due to the gap-less semiconducting nature of graphene[8] have recently been overcome by advances in the fabrication of graphene nanodevices, which allow the structural confinement of electrons. This has been achieved by tailoring (i.e. etching) graphene flakes in a desired shape,[5-7] providing a promising road to a wide range of fully functional all-graphene devices.

Here we report transport measurements on a fully tunable graphene single electron transistor (SET) as function of applied electric and magnetic fields, both strongly influencing the homogeneity and the overall transparency of the narrow graphene constrictions acting as effective tunnel barriers in the SET device. We briefly review the operation of this all graphene SET nanodevice and then we discuss in more detail the strong electric and magnetic field dependency of the overall transport. This includes the

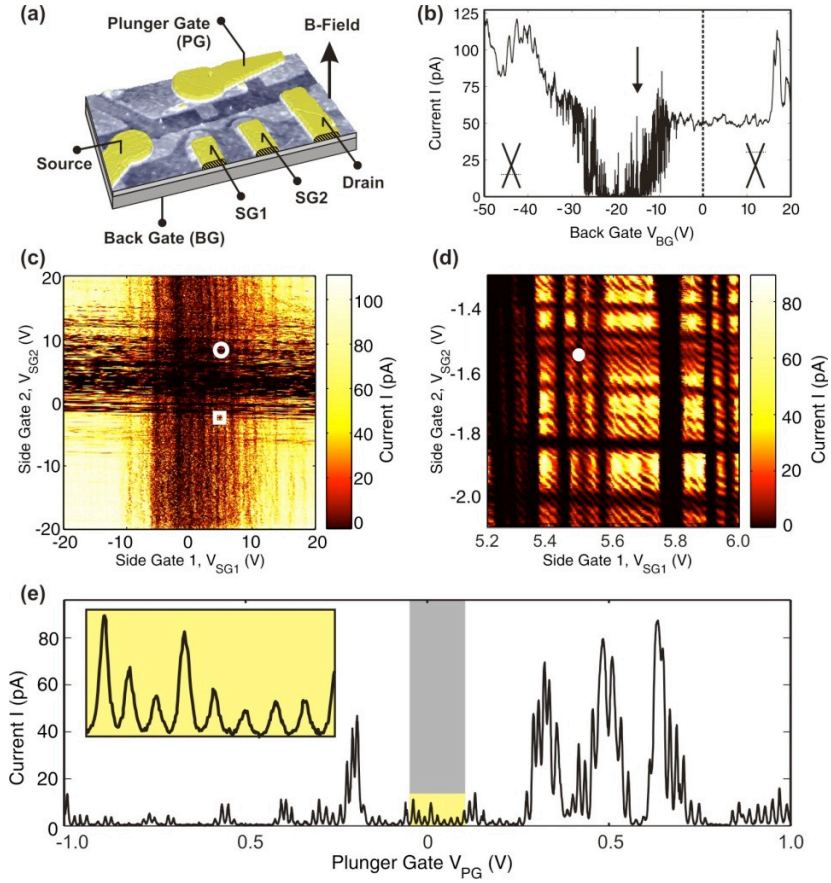

Fig. 1. (Color on line) (a) False color scanning force microscope image of the investigated graphene nanodevice. Bright areas mark the etched single layer graphene flake, whereas the elevated structures (in yellow) highlight the metal contacts. The minimum graphene feature size is approximately 50 nm. (b) Low bias back gate trace at 1.7 K and V_b = 300 µV for V_{SG1} = V_{SG2} = V_{PG} = 0 V. The resolved transport gap separates between hole and electron transport as shown by the insets. (c) Source-drain current plotted as function of V_{SG1} and V_{SG2} for constant back gate (V_{BG} = -15 V; see arrow in panel b). Here, both individual gaps can clearly be seen. (d) Close-up of panel c, as indicated therein by solid white box. On top of the horizontal and vertical transmission modulations, we observe (diagonal) Coulomb blockade resonances. (e) Source-drain current as function of the plunger gate voltage V_{PG} at fixed back gate and barrier gates in the regime shown in panel d (see white bullet). The inset (close-up) clearly shows Coulomb peaks. Partially adopted from Ref. 5.

appearance of local resonances within the narrow graphene constrictions and Coulomb resonances due to charging the lithographically defined graphene island.

2. Graphene Single Electron Transistor

The graphene single electron transistor consists of a graphene island with an area of approx. 0.06 µm^2, connected by two tunnel barriers (with width $W \approx 50$ nm) to source and drain contacts. In Fig. 1a we show a false colored 3D scanning force micrograph of

the investigated device, where both the graphene nanostructure (white) and the metal contacts (yellow) can be nicely identified. For more details on the fabrication and pre-characterization of this device please refer to Ref. 5. This device is electrostatically tunable by in total four gate electrodes, including the back gate (BG) for tuning the overall Fermi level, the plunger gate (PG) for tuning the potential on the graphene island and finally two side gates (SG1 and SG2) for adjusting both tunnel barriers (i.e. the narrow graphene constrictions) independently. All measurements have been recorded in a variable temperature insert at a base temperature of 1.7 K by lock-in techniques and a perpendicular magnetic field up to 8T has been applied. In Fig. 1b we show a characteristic low bias (V_b=300 μV < $4k_bT$) current measurement as function of applied back gate voltage. This measurement clearly shows that we can tune transport from the hole regime (left side) to the electron regime (right side) by passing through the so-called transport gap of strongly suppressed current (see region around V_{BG} = -20 V). More details on the energy scale of this transport gap can be found in Ref. 5. From now on we fix the overall Fermi energy such that we are inside the transport gap, close to the Dirac point, see vertical arrow in Fig. 1b. Since the fixed back gate voltage is slightly off-set from the center of the gap we have electrons dominating transport in the graphene source and drain leads.

By sweeping the two side gates (SG1 and SG2) independently we can now resolve two independent transport gaps (see Fig. 1c, where the dark cross corresponds to strongly suppressed current) arising from the two, spatially separated narrow graphene constrictions (sitting next to SG1 and SG2). The measured transport gap does not behave like a clean energy gap and a number of resonances can be observed inside this gap. This holds for both gaps as shown by the horizontal and vertical resonances in this panel. These resonances can also be well recognized when focusing on a smaller energy scale as shown in Fig. 1d, which is a close-up of Fig. 1c (see white box therein). However, on top of the constriction resonances we also observe resonances running diagonal clearly proving that these features are affected by both side gates almost equally. Thus, these resonances must originate from charging the central island. By further fixing the side gates (see white bullet in Fig. 1d) and finally sweeping the plunger gate we can nicely resolve Coulomb blockade peaks as shown in Fig. 1e, including the inset. The strong back ground modulations (e.g. around V_{PG} = 0.5 V) come from strong resonances in either one of the two constrictions (i.e. tunnel barriers) of the SET device. These measurements also clearly show the importance to gain deeper insights in understanding the nature of transport through these narrow graphene constrictions, which on one hand successfully act as “tunnel barriers”. However, on the other hand the local resonances strongly influence the overall single electron transport, including the actual electronic size of the island and they may also significantly contribute to the strong fluctuations in nearest neighbor peak spacing reported in recent experiments.[5,6] Moreover, these constriction resonances may become even more crucial when quantum confinement effects start to play a significant role.[7] Therefore we focus in the following (i) on the

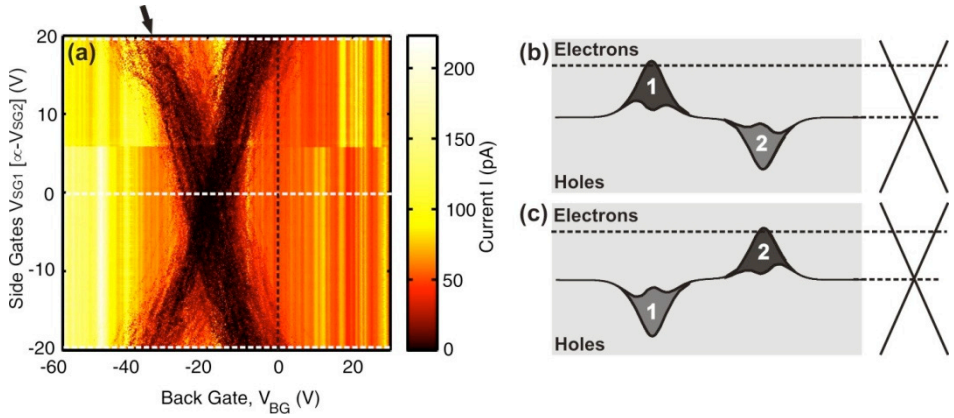

Fig. 2. (Color on line) (a) Source-Drain current at V_b = 300 μV for varying back gate voltage V_{BG} as function of asymmetric barrier gate voltages $V_{SG1} = V_{SG2}$ - 5 V. The arrow points to the slope of the transport gap associated with constriction no. 1. panel (b) and (c) illustrate the gap configuration at the upper and lower white dashed line depicted in panel (a). The black dashed lines indicate the *n*-doping level for zero back gate voltage.

homogeneity of the transport gaps and (ii) on their transparency as function of applied (perpendicular) magnetic fields.

3. Homogeneity of Transport Gaps in Graphene Constrictions

The strong tunability of this device allows studying the homogeneity of the two independent transport gaps in the constrictions in more detail. Fig. 2a shows the current measured as a function of back gate voltage (V_{BG}) and both side gates being simultaneously swept such that $V_{SG1} + V_{SG2}$ = 5 V. In comparison to Fig. 1c we can again separate between the two transport gaps (dark areas) arising from either graphene constriction 1 or 2 as depicted by the X-like structure. Here, the gap with negative slope (see also black arrow) is attributed to constrictions no. 1, whereas the gap with positive slope belongs to constrictions no. 2. In agreement with Fig. 1b we find that the overall sample for small V_{SG1} and V_{SG2} is completely *n*-doped (see also vertical dashed line in Figs. 1b and 2a). This brings an asymmetry in our system, which is also manifested in the (vertical) asymmetry (around V_{BG} = -20 V) of Fig. 2a and illustrated for two extreme cases in Figs. 2b,c. We observe that by applying a negative side gate voltage to either V_{SG1} or V_{SG2} the corresponding gap region gets stronger pushed into the electron (i.e. *n*-doped) regime leading to rather broad homogeneous transport gaps (see gaps around V_{BG} = -10 V). On the other hand, when applying positive side gate voltages we shift the region of suppressed current into the hole regime. Thus, we form locally strongly "*n*-doped" regions (including and surrounding the particular graphene constriction) in an overall *n*-doped sample leading to enhanced transport inside the gap region (less homogenous gap). In agreement with earlier experiments on a side gated graphene Hall bar,[12] we find that transport properties are strongly altered by changing the sample homogeneity in terms of local "doping" near the edges. The measurement shown in

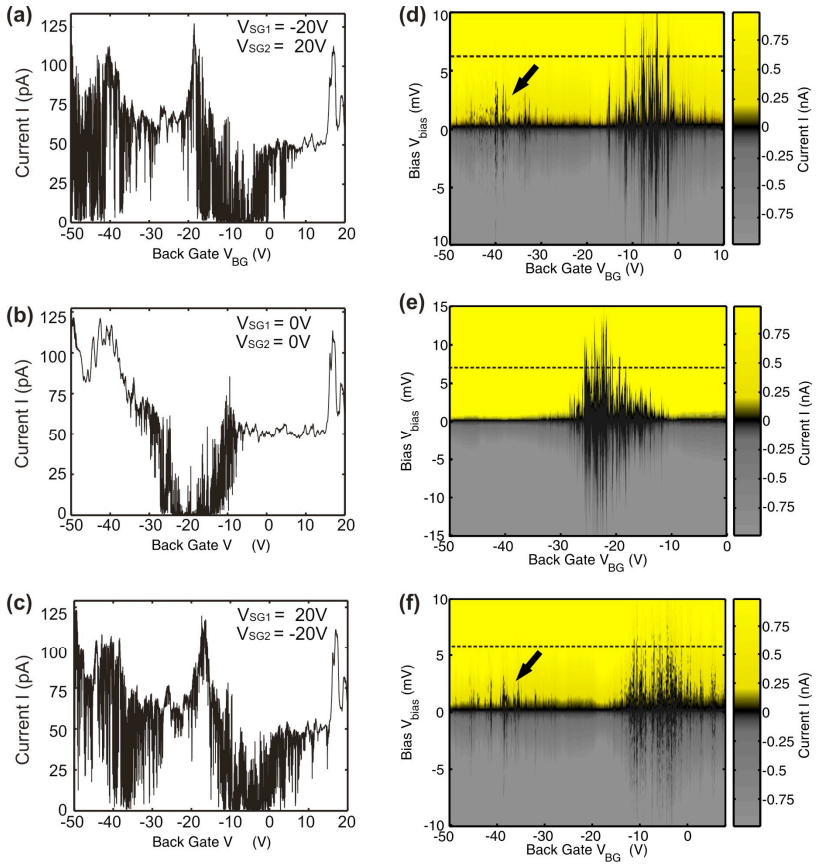

Fig. 3. (Color on line) (a-c) Low bias back gate traces at 1.7 K and V_b = 300μV for different side gate potential configurations including $V_{SG1,2}$ = 0 V, ±20 V and -(±20 V). These three traces correspond to cross-sections along the white dashed lines in Fig. 2a. (d-f) Corresponding source-drain current measurements as function of bias and back gate voltage (side gate potentials as in (a-c)). The measured effective transport gaps strongly depend on the side gate configurations. For more details see text.

Fig. 2a nicely confirms this independently for two spatially separated graphene constrictions.

In Figs. 3a-c we present three different cross-section of Fig. 2a, see white dashed lines at V_{SG1} = 20V, 0V, -20V. These measurements highlight that the homogeneity of the gap does not so much depend on the geometry (although there is also a slight asymmetry of the two constrictions arising from the sample processing as shown in Fig. 1a), but it strongly depends on the side gate potential configuration. This is confirmed by high bias measurements in order to energetically resolve the independent transport gaps as shown in Figs. 3d-f. In good agreement with earlier work,[5] the energy scales of the measured (rather homogenous) transport gap agrees reasonably well with theoretical models[13] based on the formation of quantum dots along the narrow graphene constrictions only

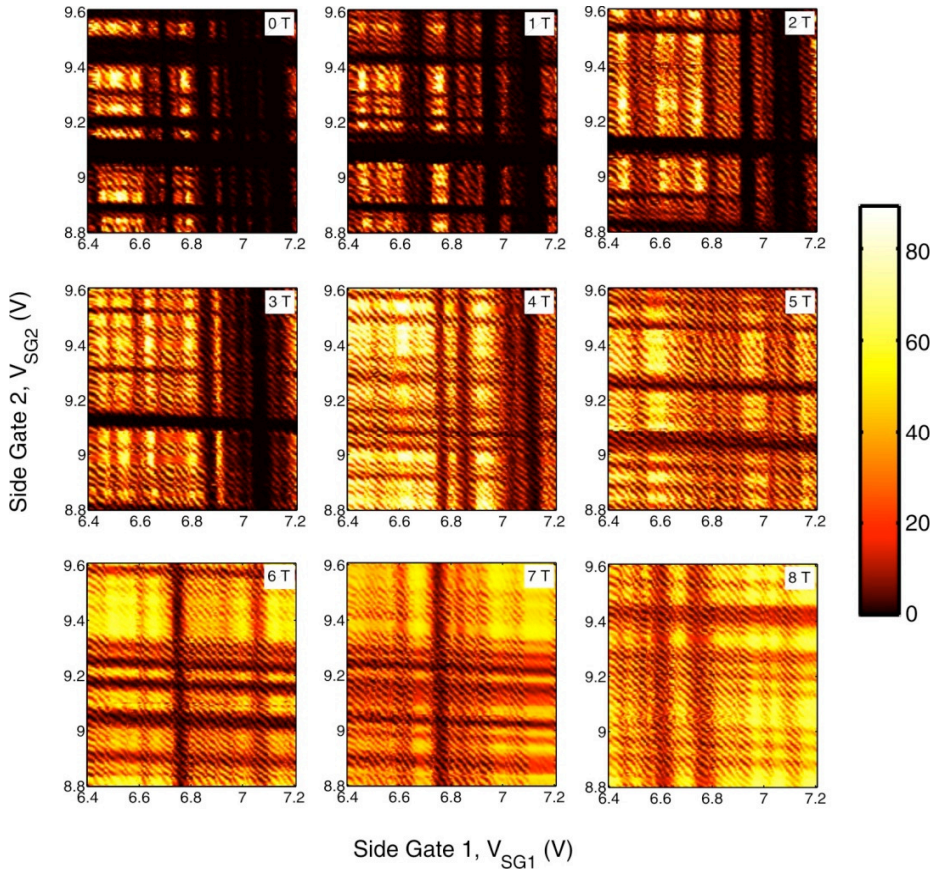

Fig. 4. (Color on line) Source-drain current measurements plotted as function of V_{SG1} and V_{SG2} for different perpendicular magnetic fields (see different labels in these panels). These measurements have been taken for a constant V_{SG1} - V_{SG2} parameter range and a fixed back gate voltage of V_{BG} = -15 V and V_b = 300 μV. The overall transparency of the transport gap clearly increases with increasing magnetic field as seen from the generally increased conductance level.

depending on the width *W* of the constriction (see dashed lines in Figs. 3d-f at 6.5 meV). Nevertheless, the measurements presented here make clear that this cannot be the end of this story since we observe a strong dependence on the sample homogeneity, where this simple model does not hold to approximate the gap size (see e.g. arrows in Figs. 3d,f).

4. Transport Gap Transparency as Function of Magnetic Field

After having discussed the transport gap homogeneity depending on local electrostatic "doping" we now turn to the electron transport dependency as function of a perpendicular applied magnetic field (see arrow in Fig. 1a). In Fig. 4 we show a close up of Fig. 1c (see white circle therein) for a series of different magnetic fields up to B_{max}= 8 T. In these panels we again clearly observe resonances which can be attributed to either graphene

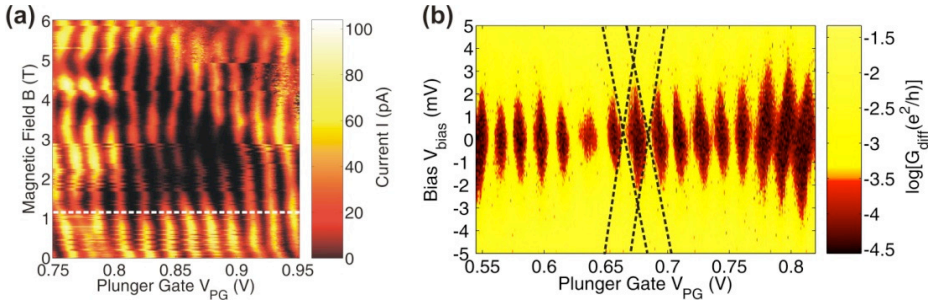

Fig. 5. (Color on line) (a) Coulomb blockade peaks measured at V_b = 300 µV (and V_{SG1} = 6.878 V, V_{SG2} = 9.381 V) as function of stepped magnetic field. This "spaghetti"-like pictures provide indications of strong orbital effects. (b) Corresponding Coulomb diamonds in differential conductance G_{diff}, represented in a logarithmic color scale plot (dark regions represent low conductance) at a constant magnetic field of B = 1.125 T (see white dashed line in panel (a)).

constriction no. 1 (vertical lines) or to constriction no. 2 (horizontal lines) and on top we identify a large number of almost equally spaced Coulomb blockade resonances.

Although our measurements do not allow to track individual resonances when moving from low to high magnetic fields, which might be mainly due to some instabilities of our sample, we can clearly see that the overall signatures of local resonances in both constrictions and Coulomb oscillations do not disappear for increasing magnetic fields. Additionally, we observe the overall trend of an increasing transport gap transparency as increasing magnetic field. Moreover, it is interesting to note that for larger magnetic fields (B = 4-8 T) the maximum current seems to saturate and it is limited to a smaller value as compared to measurements performed at lower magnetic fields (compare e.g. the panels 2 T, 4 T, and 8 T in Fig. 4). By focusing on a few individual Coulomb blockade peaks as show in Fig. 5a we observe strong orbital effects of the magnetic field on the position of the individual Coulomb peaks, where the fluctuations are clearly exceeding the peak spacing, which can be related to an energy scale of approx. 3.5meV.[5] This should become pronounced when the characteristic magnetic length[14] $l(B) = \hbar\, v_F / B^{½} \approx 25.7$ nm/$(B/tesla)^{½}$ significantly exceeds the smallest length scale of the graphene constrictions of $W \approx 50$, thus for B-fields exceeding 0.3 T. This is in reasonably good agreement with the measurements presented in Fig. 5a where a qualitative change can be "imagined" around 0.3 T. These large energy scales exclude any spin effects and are attributed to orbital effects leading to this "spaghetti"-like pattern with an additional strong amplitude modulation along the B-field direction. Finally, we present in Fig. 5b characteristic Coulomb diamond measurements, i.e. measurements of the differential conductance ($G_{diff} = dI/dV_b$) as a function of bias voltage V_b and plunger gate voltage V_{PG} for an applied magnetic field of B = 1.125 T clearly showing that the charging energy of the graphene island is not significantly modified as function of the magnetic field. From these measurements we extract a charging energy of approx. 3.5 meV, which agrees with the lithographically defined area of the graphene island and with measurements at zero magnetic field as presented in Ref. 5.

5. Conclusion

In conclusion, we have investigated a fully tunable graphene single electron transistor based on an etched graphene nanostructure with lateral graphene gates. Its functionality was demonstrated by observing electrostatic control over the tunneling barriers. We focused here on the transport gap homogeneity arising from the two spatially separated narrow graphene constrictions and on the transport transparency as function of magnetic field. We find that the size of the effective energy gap opened by graphene nano constrictions is not only a function of geometry, but it also strongly depends on the local gating. In addition we have shown that the overall electron transport transparency increases with increasing magnetic field. These results give detailed insights into narrow graphene constrictions, which are important for tunable graphene quantum dot devices and open the way to study the microscopic physics relevant for the gap formation and more general it opens to door to tunable graphene quantum dots with smaller dimensions.

Acknowledgments

The authors wish to thank R. Leturcq, P. Studerus, C. Barengo, P. Strasser, S. Schnez, A. Castro Neto and K. S. Novoselov for helpful discussions. Support by the ETH FIRST Laboratory and financial support by the Swiss National Science Foundation and NCCR nanoscience are gratefully acknowledged.

References

1. Z. Chen, Y. Lin, M. Rooks, P. Avouris, *Physica E* **40**, 228 (2007).
2. M. Y. Han, B. Özyilmaz, Y. Zhang, P. Kim, *Phys. Rev. Lett.* **98**, 206805 (2007).
3. X. Li, X. Wang, L. Zhang, S. Lee, H. Dai, *Science* **319**, 1229 (2008).
4. S. Russo, J. B. Oostinga, D. Wehenkel, H. B. Heersche, S. S. Sobhani, L. M. K. Vandersypen, A. F. Morpurgo, *Phys. Rev. B* **77**, 085413 (2008).
5. C. Stampfer, J. Güttinger, F. Molitor, D. Graf, T. Ihn, K. Ensslin, *Appl. Phys. Lett.* **92**, 012102 (2008); C. Stampfer, E. Schurtenberger, F. Molitor, J. Güttinger, T. Ihn, K. Ensslin, *Nano Lett.* **8(8)**, 2378 (2008).
6. L. A. Ponomarenko, F. Schedin, M. I. Katsnelson, R. Yang, E. H. Hill, K. S. Novoselov, A. K. Geim, *Science* **320**, 356 (2008).
7. S. Schnez, F. Molitor, C. Stampfer, J. Güttinger, I. Shorubalko, T. Ihn, K. Ensslin, arXiv:0807.2710v2 (2008).
8. For review see please: A. K. Geim, K. S. Novoselov, *Nat. Mater.* **6**, 183 (2007).
9. H. Min, J. E. Hill, N. A. Sinitsyn, B. R. Sahu, L. Kleinman, A. H. MacDonald, *Phys. Rev. B* **74**, 165310 (2006).
10. D. Huertas-Hernando, F. Guinea and A. Brataas, *Phys. Rev. B* **74**, 155426 (2006).
11. B. Trauzettel, D. V. Bulaev, D. Loss, G. Burkard, *Nature Physics* **3**, 192 (2007).
12. F. Molitor, J. Güttinger, C. Stampfer, D. Graf, T. Ihn, K. Ensslin, *Phys. Rev. B* **76**, 245426 (2007).
13. F. Sols, F. Guinea, A. H. Castro Neto, *Phys. Rev. Lett.* **99**, 166803 (2007).
14. J. Schliemann, *New J. Phys.* **10**, 043024 (2008).